

A Stochastic Modeling Approach of Quantized Systems with Application to Fault Detection and Isolation of an Automotive Electrical Power Generation Storage System

Sara Mohon¹ and Pierluigi Pisu²

^{1,2}*Clemson University International Center for Automotive Research, Greenville, South Carolina, 29607, USA*

smohon@clemson.edu

pisup@clemson.edu

ABSTRACT

This paper introduces a stochastic modeling approach for a quantized system for the purpose of fault detection and isolation in an automotive alternator system. Three common alternator faults including belt slip, diode failure, and incorrect reference voltage for the voltage controller are considered and analyzed. A continuous nonlinear model of the alternator system is quantized into discrete states in order to simplify diagnostic efforts. The paper describes a stochastic modeling approach that creates a time-varying probability transition matrix that can be computed in real-time without the need for Monte Carlo simulation. Fault detection and isolation occurs through comparison of the most probable state from the transition matrix and the quantized output state.

1. INTRODUCTION

Today's vehicles require higher electrical demands than ever before due to more mandated safety technology and popular consumer technology integrated within the vehicle. The purpose of the vehicle's electrical power generation storage (EPGS) system is to maintain the necessary electrical power needed to start the vehicle and keep it running smoothly. A healthy EPGS system is crucial for proper operation of a vehicle.

Faults within the EPGS system do occur with age. Typical faults include belt slippage between the engine crankshaft and alternator pulley, failure of a diode in the bridge diode rectifier, and change in reference voltage of the voltage controller. These faults however can be detected and isolated with a carefully chosen diagnostic algorithm.

Diagnostics of the EPGS system is important for the vehicle owner and mechanic. Early diagnostics of a faulty EPGS system can warn the owner that the vehicle needs repair

Sara Mohon et al. This is an open-access article distributed under the terms of the Creative Commons Attribution 3.0 United States License, which permits unrestricted use, distribution, and reproduction in any medium, provided the original author and source are credited.

before more costly damage to other components occur. Early detection saves the owner further loss of time and money for repair. Furthermore, diagnostics stored in a vehicle's electronic control unit can be accessed by a mechanic to quickly and effectively determine the problem and steps needed to solve it.

Scacchioli, Rizzoni, and Pisu (2006) proposed a fault isolation approach for an EPGS system using two equivalent alternator models. One equivalent model for a healthy alternator and one equivalent model for an alternator with one broken diode. Parity equations and three residuals with constant thresholds were used for fault isolation. The approach assumed a 3000 second Federal Urban Driving Schedule (FUDS) cycle.

Zhang, Uliyar, Farfan-Ramos, Zhang, and Salman (2010) proposed a fault isolation approach for an EPGS system using parity relations trained by Principal Component Analysis (PCA). Three residuals with constant thresholds were used for isolation. The approach assumed a staircase profile for both load current and alternator speed input, which is not a realistic scenario.

Hashemi and Pisu (2011) proposed a fault isolation approach for an EPGS system using two observers and three residuals. The approach assumed a staircase profile for load current and a portion of the FUDS cycle for alternator speed. Adaptive thresholds were used for isolation. In other similar work, Hashemi and Pisu (2011) showed the same approach but created a reduced order adaptive threshold model using Gaussian fit of data. The second approach was less computationally intensive.

Scacchioli, Rizzoni, Salman, Onori, and Zhang (2013) proposed a fault isolation approach for an EPGS system using one equivalent EPGS model that used parity equations to produce three residuals for fault isolation. The approach used a staircase profile for both load current and alternator speed input.

As stated, previous work for fault isolation in an EPGS system has included observers and parity relations. The approaches with observers were built for linear systems that approximate the nonlinear behavior of the EPGS system. These approaches cannot be extended for direct use on the nonlinear system itself. At least three residuals are required for all previous approaches. It is also concerning that some approaches were not validated using real driving situations. Therefore these approaches have limited scopes.

In this paper, the EPGS system is modeled as a quantized system. The motivation for using a quantized system stems from the qualitative change in system behavior during EPGS faults and the need for a simpler real-time diagnostic algorithm. The approach in this paper uses a time-varying probability transition matrix and only one residual to detect and isolate faults. The approach requires much less real-time computational effort than previous works, which required at least 3 residuals. EPGS system data was created using a portion of the FUDS cycle to emulate a real-world situation. This approach is shown here in the context of an EPGS system but could be used for diagnostics in other systems as well including nonlinear systems.

The first section of this paper describes the EPGS model and an approximation of this model named the Equivalent EPGS model. The second section discusses three common faults in the model and how each affects the model output. The third section introduces the general concept of a stochastic model of a quantized system for the purpose of fault detection. The fourth section describes a new method to calculate the probability transition matrix for a quantized EPGS system. The last section provides simulation assumptions and results for each of the three faults in the EPGS system.

2. EPGS MODEL AND EQUIVALENT EPGS MODEL

This paper analyzes the EPGS system shown in Figure 1 as modeled by Scacchioli et al. (2006). It consists of a voltage controller, alternator, and battery. The controller can be an electronic control unit or a voltage controller on the alternator itself. In this paper, the controller is a part of the alternator to regulate field voltage. The alternator model consists of an AC synchronous generator, three phase full bridge diode rectifier, voltage controller, and excitation field.

The engine crankshaft mechanically spins the generator's rotor by use of a belt and pulley. The rotor is a ferrous metal wrapped with a single conductive winding. When the controller applies a small field voltage to the winding, a small field current flows through the winding. The flow of current through the winding produces a magnetic rotor with a north and south pole. However, the stator is composed of three phase stationary windings. As the magnetic rotor moves relative to the conductive stator windings, an electromotive force is induced in the stator windings. If the

stator windings are connected to an electrical load, then AC current will flow in each of the three stator windings. The three currents are sent to a diode bridge rectifier to produce DC current for electrical loads or for recharging the battery. Therefore, the alternator takes mechanical energy of the engine and produces electrical energy for the battery or loads of the vehicle.

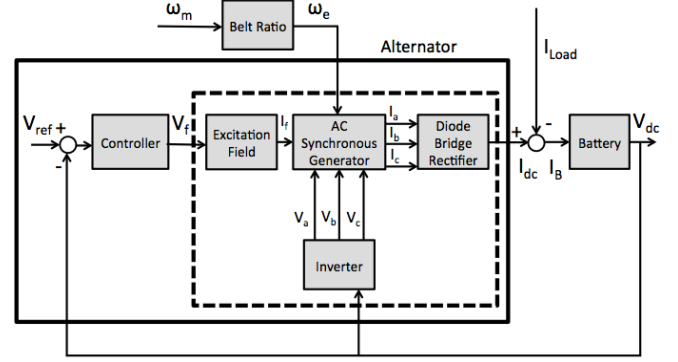


Figure 1. EPGS model

The model for the EPGS system results in a complex nonlinear system but can be more easily modeled by an equivalent DC electric machine as described by Sacchioli et al. (2006). The dashed line in Figure 1 encompasses the components represented by the DC model. This approximation gives the equivalent EPGS model shown in Figure 2.

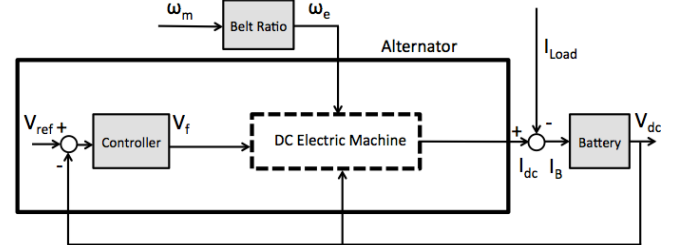


Figure 2. Equivalent EPGS model

The DC electric machine is modeled by the state space system in Eq. (1) as shown by Hashemi (2011).

$$\begin{bmatrix} \dot{z}_1 \\ \dot{z}_2 \end{bmatrix} = \begin{bmatrix} 0 & a_{12}(\omega_e) \\ 1 & a_{22}(\omega_e) \end{bmatrix} \begin{bmatrix} z_1 \\ z_2 \end{bmatrix} + \begin{bmatrix} b_{11}(\omega_e) & b_{12}(\omega_e) & b_{13}(\omega_e) \\ 0 & b_{22}(\omega_e) & b_{23}(\omega_e) \end{bmatrix} \begin{bmatrix} u_1 \\ u_2 \\ u_3 \end{bmatrix} \quad (1)$$

$$y = \begin{bmatrix} 0 & 1 \end{bmatrix} \begin{bmatrix} z_1 \\ z_2 \end{bmatrix}$$

Equation (1) has two states z_1 and z_2 and inputs u_1 , u_2 , and u_3 . The system inputs represent the alternator field voltage V_f , angular frequency of alternator ω_e , and dc voltage of the battery V_{dc} also shown in Eq. (2). The coefficients a_{12} , a_{22} and $b_{11} \dots b_{23}$ are functions of engine speed and were found using system identification by Hashemi (2011) using test data at different constant engine speeds. In this model, state z_2 is the measurable quantity I_{dc} which is the rectified output current of the alternator.

$$\begin{aligned}
 y_2 &= I_{dc} = z_2 \\
 u_1 &= V_f \\
 u_2 &= \omega_e \\
 u_3 &= V_{dc}
 \end{aligned}
 \tag{2}$$

3. POSSIBLE FAULTS IN EPGS SYSTEM

The EPGS system is important in every vehicle and faults in the system need to be detected and isolated as quickly as possible to prevent costlier damage. This paper considers three common faults that occur in an EPGS system. Possible fault locations in EPGS system are bolded in Figure 3.

1. *Voltage controller fault:* This fault occurs when the reference voltage V_{ref} is incorrectly raised or lowered by a percentage of the nominal V_{ref} . The fault can cause the alternator to overcharge or undercharge the battery.
2. *Open diode rectifier fault.* This fault occurs when a diode in the diode bridge rectifier breaks. The fault results in a large ripple in battery voltage V_{dc} and alternator output current I_{dc} thereby decreasing the efficiency of alternator output.
3. *Belt slip fault.* This input fault occurs when the belt between the engine crankshaft and alternator pulley slips due to insufficient tension. The belt slip causes a decrease in alternator rotational speed ω_e and a decrease in alternator output voltage. To compensate, the voltage controller increases the field voltage and/or the battery must discharge more often to meet load demand. This can age the battery prematurely. Belt slip can signify the belt is worn and needs to be replaced.

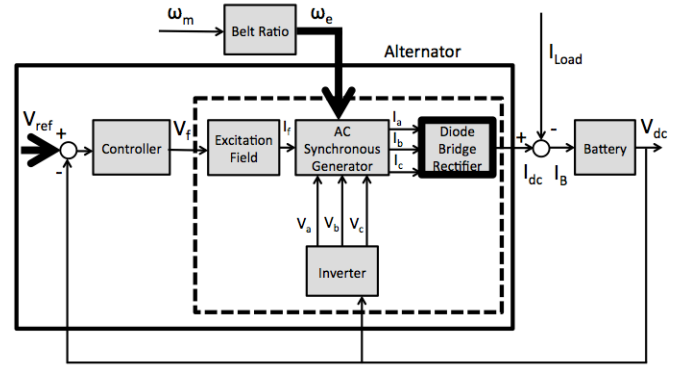


Figure 3. Possible faults in EPGS model

4. STOCHASTIC MODEL FOR QUANTIZED SYSTEM

Equation 1 gives the continuous model of the DC electric machine. A continuous system provides much more information than a discrete system for a diagnostic algorithm to sift through to find a fault. If a continuous system could be simplified in a discrete manner without significant loss of information, the diagnostic algorithm will have a simpler task when searching for a fault.

Suppose we diagnose a continuous system as a quantized system shown in Figure 4 (Blanke, Kinnaert, Lunze, and Staroswiecki, 2006). Input $u(t)$ is the continuous input at time t , $f(t)$ is the amount of fault at time t , and $y(t)$ is the output at time t . The output $y(t)$ passes through a quantizer and produces $[y(t)]$. The real valued signal $y(t)$ is assigned a new name $[y(t)]$ that corresponds to an interval of real valued signals given a set of real valued intervals. For example, if $y(t=10)=70$ and the interval of real values 50 through 75 is assigned the name $[y(t=10)]=2$, then $y(t=10)$ will be assigned the quantized name of 2.

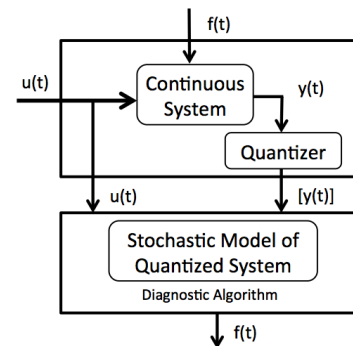


Figure 4. Diagnostics of quantized system

Assuming output $y(t)$ contains two observable outputs $y_1(t)$ and $y_2(t)$ that can be quantized, a plot of y_2 vs y_1 can be visualized as a set of rectangles as shown in Figure 5. Output $y_1(t)$ can be quantized into intervals a-e and output $y_2(t)$ can be quantized into intervals 1-5. The grey section represents the system space. As input $u(t)$ continuously

changes over time, the discrete output $[y(t)]$ will transition from one grey rectangle to another. Some rectangles will be more favorable for a system to move into for a given input and a current rectangle. The unfavorable rectangle transitions can be interpreted as having a low probability of occurrence. Transition probabilities from one rectangle to another could be arranged in a probability transition matrix and could be very useful for diagnostics. If a transition occurs that has very low probability, then a fault may be present.

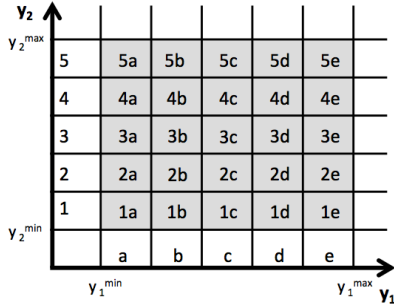


Figure 5. Example of quantizing two outputs

A typical approach to obtain a static probability transition matrix entails using a healthy model of the plant and the use of Monte Carlo simulation as shown by Alam (1995). In this paper, a new method for obtaining a time-varying probability transition matrix while monitoring the data for faults is introduced in the next section in application to the DC electric machine.

5. NEW METHOD FOR PROBABILITY TRANSITION MATRIX

Using Eq. (1) the DC electric machine system can be viewed as a 2D space with z_1 and z_2 axes. The system output will be contained on this plane. Since z_2 is the only output, the user knows where the output is in relation to the z_2 axis. The user does not know where the output is in relation to the z_1 axis except that it must exist between some minimum value z_1^{min} and maximum value z_1^{max} shown in Figure 6.

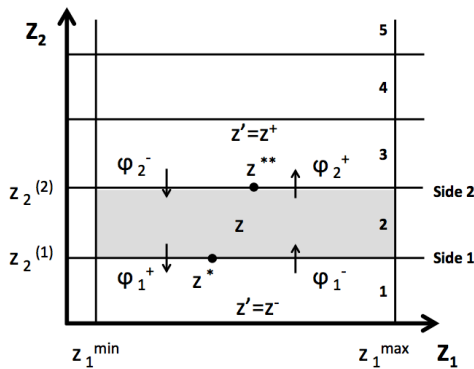


Figure 6. Graph of quantized DC electric machine system with flow definitions

For the purpose of diagnostics, the system space is divided into quantized states across the z_2 axis and assigned names such as 1, 2, 3, etc. as shown on right hand side in Figure 6. In this paper, the user assumes that with each event, in this case one time step, the current state z can only transition up or down to an adjacent state z' or remain in the same state z . The state may not jump over other states to nonadjacent states. The state may not move left or right outside of the z_1 boundaries. The selection of state boundaries will depend on the system being investigated to ensure only adjacent states are used by the system in healthy conditions.

The objective is to calculate the probability of transitioning out of current state z and the probability of future state $z' = z$. The probabilities are calculated using a two-dimensional form of the divergence theorem. The three-dimensional form of the divergence theorem is defined in Eq. (3). We define V as a closed volume, A as the surface area of V , \vec{n} as the outward pointing normal vector of the closed volume V , and \vec{F} as a continuously differentiable vector field in volume V . A picture for a cubic volume is shown in Figure 7.

$$\iiint_V (\nabla \cdot \vec{F}) dV = \iint_A (\vec{F} \cdot \vec{n}) dA \tag{3}$$

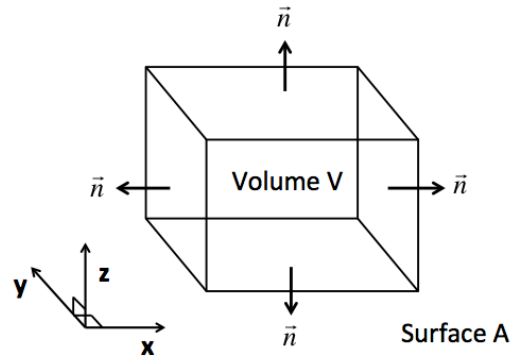


Figure 7. Graph of 3D Divergence Theorem

For the alternator problem, one can imagine multiple cubes stacked in the z direction and then collapsing the picture to only contain the x - z plane. This yields the 2D space with desired upward and downward flow consistent with the alternator problem in Figure 6.

A two-dimensional form of the divergence theorem is defined in Eq. (4). We define C as a closed curve, A as the 2D region in the plane enclosed by C , \vec{n} as the outward pointing normal vector of the closed curve C , and \vec{F} as a continuously differentiable vector field in region A . A graph of the 2D divergence theorem for the alternator problem is shown in Figure 8.

$$\iint_A (\nabla \cdot \vec{F}) dA = \int_C (\vec{F} \cdot \vec{n}) dr \quad (4)$$

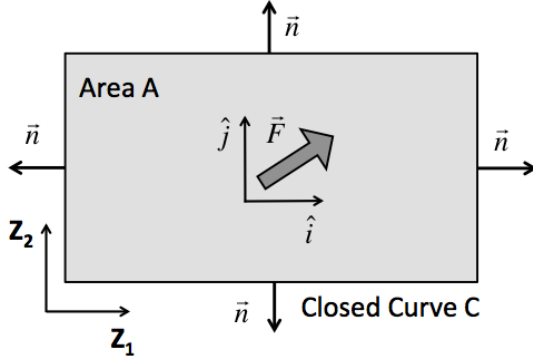


Figure 8. Graph of 2D Divergence Theorem for state z in DC electric machine state space

We consider that the vector field \vec{F} describes transition flow in and out of the current state along the state boundaries. For the DC electric machine model, \vec{F} is defined as Eq. (5) where \hat{i} and \hat{j} are coordinates of vector field F and functions f_1 and f_2 are defined by states z_1 and z_2 from the state space model in Eq. (1).

$$\begin{aligned} \vec{F} &= f_1 \hat{i} + f_2 \hat{j} \\ \dot{z}_1 &= f_1(z_1, z_2, u_1, u_2, u_3) \\ \dot{z}_2 &= f_2(z_1, z_2, u_1, u_2, u_3) \end{aligned} \quad (5)$$

The flow through the left and right sides of the area A in Figure 8 will be assumed zero for the alternator problem. The line integrals along the state boundaries shown in Figure 6 will determine flow in and out of the state. Flow out of state z is defined as a positive value φ^+ and flow into state z is a negative value φ^- . Since each side may have flow in and flow out sections, the flow transition point z^{**} or z^* is found if necessary and the appropriate limits of integration for flow in and flow out are integrated for each side. Transition points are shown in Figure 6. Without loss of generality assume $f_2 < 0$ if $z_1 < z^*, z^{**}$ and $f_2 > 0$ if $z_1 > z^*, z^{**}$ such that Eq. (6) holds. The upward and downward flow through each side of state z is given by Eq. (7).

$$\begin{aligned} f_2(z^*, z_2^{(1)}, u_1, u_2, u_3) &= 0 \\ f_2(z^{**}, z_2^{(2)}, u_1, u_2, u_3) &= 0 \end{aligned} \quad (6)$$

$$\begin{aligned} \varphi_1^+ &= - \int_{z_1^{\min}}^{z_1^*} f_2(z_1, z_2^{(1)}, u_1, u_2, u_3) dz_1 > 0 \\ \varphi_1^- &= - \int_{z_1^*}^{z_1^{\max}} f_2(z_1, z_2^{(1)}, u_1, u_2, u_3) dz_1 < 0 \\ \varphi_2^- &= \int_{z_1^{\min}}^{z_1^{**}} f_2(z_1, z_2^{(2)}, u_1, u_2, u_3) dz_1 < 0 \\ \varphi_2^+ &= \int_{z_1^{**}}^{z_1^{\max}} f_2(z_1, z_2^{(2)}, u_1, u_2, u_3) dz_1 > 0 \end{aligned} \quad (7)$$

Next we define φ_{in} , φ_{out} , and φ_{total} in Eq. (8) in order to build probabilities. The sum of the absolute value of all inward flow is defined as φ_{in} . The sum of all outward flow is defined as φ_{out} . The total flow φ_{total} is the sum of φ_{in} and φ_{out} .

$$\begin{aligned} \varphi_{in} &= |\varphi_1^- + \varphi_2^-| \\ \varphi_{out} &= \varphi_1^+ + \varphi_2^+ \\ \varphi_{total} &= \varphi_1^+ + |\varphi_1^-| + |\varphi_2^-| + \varphi_2^+ \end{aligned} \quad (8)$$

The value φ_{net} is the sum of all flows along the boundaries of state z without the use of absolute values. A positive value of φ_{net} represents a net outward flow out of state z . A negative value of φ_{net} represents a net inward flow into state z . The sum of the flows along the boundary of state z is given by Eq. (9).

$$\varphi_{net} = \varphi_1^- + \varphi_1^+ + \varphi_2^+ + \varphi_2^- \quad (9)$$

While the sign of φ_{net} is important to determining if current state z will transition to a new state, it does not contain information about which state it transitions to. Instead, careful manipulation of Eq. (8) builds transition probabilities through each side.

The notion of probability can be interpreted as counting types of occurrences and then normalizing the count of each type by the total occurrences. Suppose the occurrences of outward and inward flow defined in Eq. (7) are normalized by the total flow defined in Eq. (8). For example, the probability to transition up will be defined as the outward flow through side 2, φ_2^+ , divided by the total flow φ_{total} . We can then define z^+ as the state above current state z and define z^- as the state below current state z . Equation (10) gives the probability to stay within the current state and the probability to transition up or transition down to an adjacent state. Uniform probability distribution is assumed along the borders of each state.

$$1 = \frac{\varphi_{in}}{\varphi_{total}} + \frac{\varphi_{out}}{\varphi_{total}}$$

$$1 = \frac{|\varphi_1^- + \varphi_2^-|}{\varphi_{total}} + \frac{\varphi_2^+}{\varphi_{total}} + \frac{\varphi_1^+}{\varphi_{total}} \quad (10)$$

$$1 = \Pr(z' = z | z) + \Pr(z' = z^+ | z) + \Pr(z' = z^- | z)$$

At each time step the probability to stay or transition up or transition down is calculated using the current state boundaries and the current input. This information builds a time-varying probability transition matrix named L that can be constructed as shown in Table 1 for the example of current state $z=2$ at time t .

Table 1. Example of probability transition matrix L for current state $z=2$ at a time t

		Future State z'			
		1	2	3	4
Current State z	1	0	0	0	0
	2	$\Pr(z' = z^- z)$	$\Pr(z' = z z)$	$\Pr(z' = z^+ z)$	0
	3	0	0	0	0
	4	0	0	0	0

6. SIMULATION RESULTS

Previous work by Scacchioli et al. (2006) yielded a complete nonlinear EPGS model. This nonlinear model uses ω_e , I_{load} , and V_{ref} as inputs and yields V_f , V_{dc} , and battery dc current I_{dc} as output as shown in Figure 9.

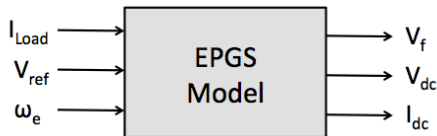


Figure 9. Schematic of EPGS model

Diagnostics for the belt fault case, diode fault case, and voltage controller fault case are accomplished by using the EPGS model and the new method for the probability transition matrix L. The EPGS output I_{dc} is quantized and sent to the flow calculator. The flow calculator uses the outputs of EPGS model and the f_2 equation from the DC electric machine model to calculate the flow φ through each side of the current quantized state. The flow and current quantized state are used to construct the probability transition matrix L. The quantized state and probability

transition matrix L are used in diagnostics for fault detection and isolation. The procedure is illustrated in Figure 10.

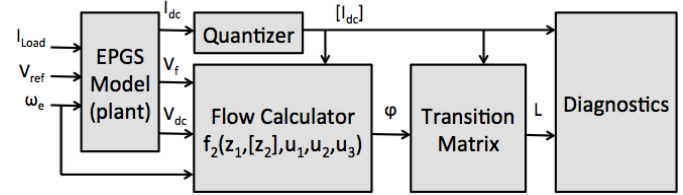


Figure 10. EPGS model with diagnostics

The following parameters were used to craft the inputs for a nonlinear EPGS Simulink model.

1. Simulate vehicle driving 289 seconds of FUDS cycle compressed to 72 seconds during simulation.
2. Simulation time step is $1e-4$ seconds.
3. Tire radius of vehicle is 0.391 meters.
4. Final drive gear ratio is 4.72:1.
5. Belt ratio of 2.92 between engine crankshaft and alternator pulley.
6. Reference battery voltage V_{ref} is a constant 14.46 volts.
7. Current load profile is a square wave shown in Figure 11.

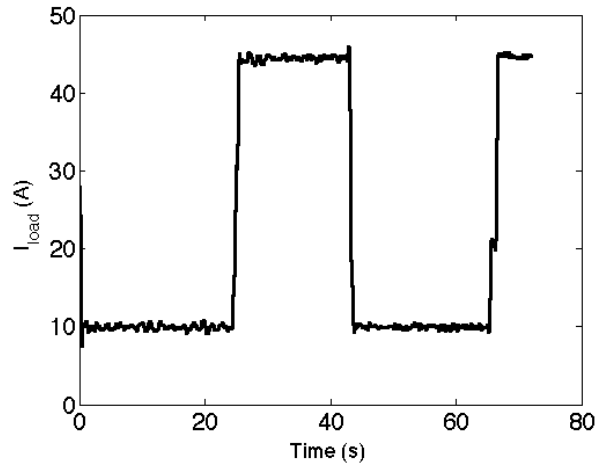


Figure 11. Current load profile

Using the aforementioned assumptions, ω_e can be easily calculated and is shown in Figure 12. The V_{dc} and V_f outputs of the EPGS model are given in Figure 13 and 14 respectively. The V_{dc} and V_f data will be used as inputs for the DC electric machine model but were downsampled to time step of 0.1 seconds.

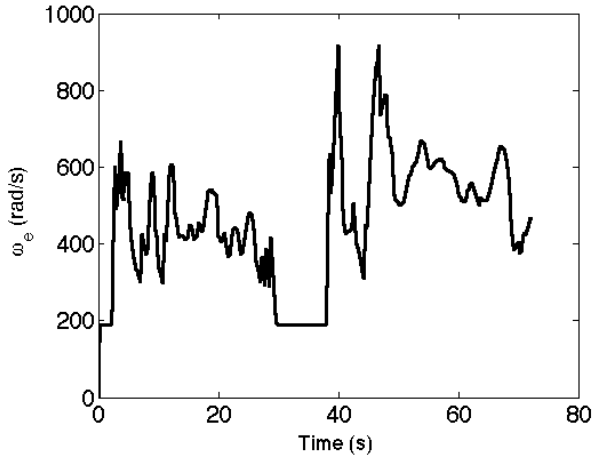


Figure 12. Alternator rotational speed input

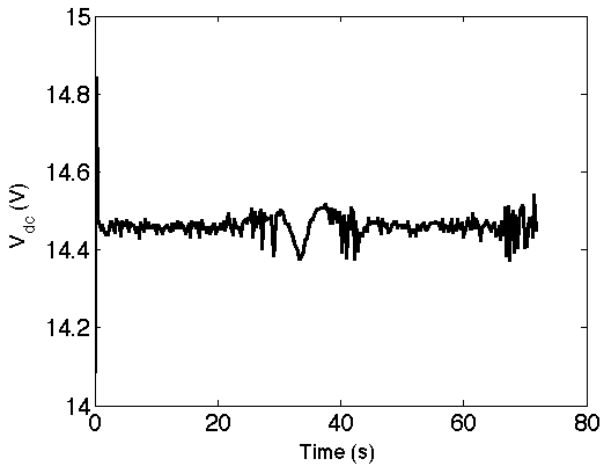


Figure 13. Battery DC voltage input

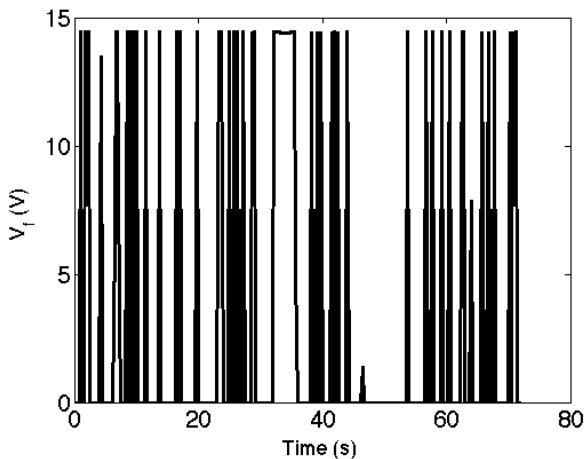


Figure 14. Alternator field voltage input

Figures 12, 13, and 14 represent the nominal inputs to the DC electric machine model to which faults will be injected.

Table 2 details the selected injection time and magnitude of fault relative to nominal that were injected during simulation. In other words, the nominal inputs were modified to simulate a fault.

Table 2. Fault injection time and magnitude

Fault	Injection time (s)	Modified Input	Resulting % drop with respect to nominal
Belt Slip	10	ω_e	0.8
Open Diode	10	V_{dc}	one broken diode
Voltage Controller	10	V_{ref}	0.3

Output z_2 range for nominal and faulty cases must be quantized into rectangles to find the probability transition matrix over time. Output z_2 is quantized into 12 states with names 1-12. The same boundaries and names will be used for faulty cases as well.

The z_1 range for this simulation is z_1^{\min} is $-2.210e+06$ and z_1^{\max} is $6.683e+06$. Given the z_1 range, the quantized states, and u_1 , u_2 , and u_3 , the probability transition matrix can now be calculated using the f_2 function from Eq. (1).

The probability transition matrix L contains the prediction of the most likely quantized state $z' = z_L$ and its probability $P(z' = z_L)$ at the next time step. The most likely probability and most likely predicted state can be compared with the quantized output state $[I_{dc}]$ that actually occurs. If there is a relatively high probability of a particular state transition occurring and that state transition does not occur, then a fault may be present. An example of the most likely transition probabilities, most likely states, and output states over time for belt fault case is shown in Figure 15.

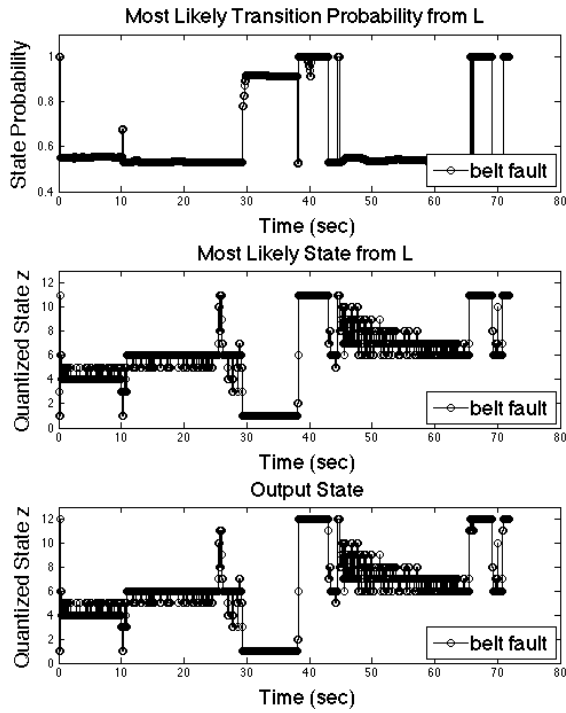


Figure 15. Belt fault outputs

Disagreement between predicted and output states are clear after calculating the difference of quantized output state $[I_{dc}]$ and the predicted state from probability transition matrix L . This difference is defined as the residual r in Eq. (11). The residual results for each fault case are shown in Figures 16, 17, and 18.

$$r = [I_{dc}] - z_L \quad (11)$$

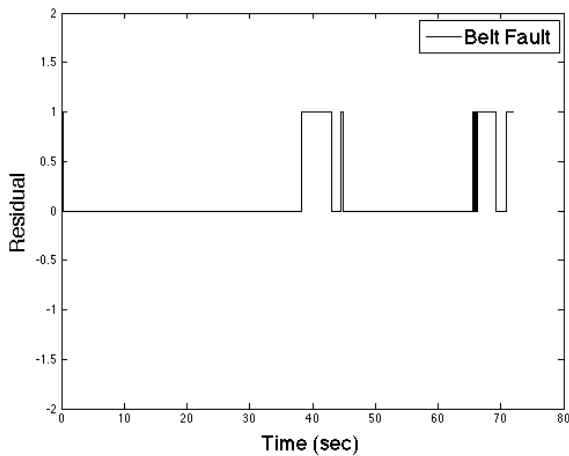


Figure 16. Belt fault residual

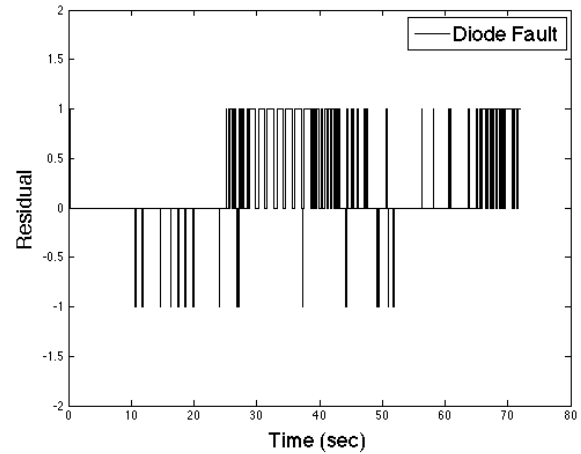


Figure 17. Diode fault residual

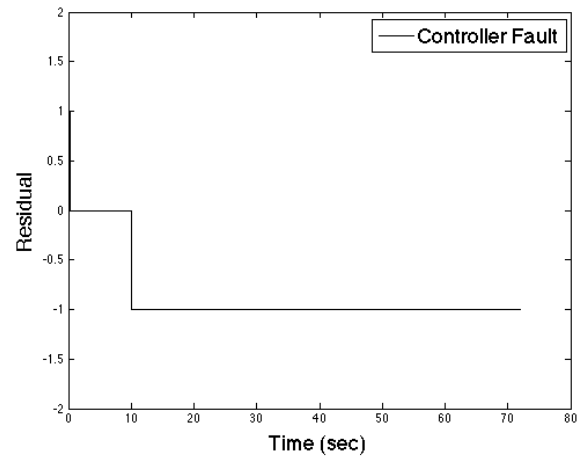


Figure 18. Voltage controller fault residual

All three fault cases show a short-term disagreement $r \neq 0$ between predicted and output states at time $t=0.2$ seconds but returns to agreement $r = 0$ immediately at $t=0.3$ seconds. The disagreement occurs before a fault is injected at time $t=10$ seconds. This disagreement at $t=0.2$ could trigger a false alarm during fault detection. Similar rapid switching behavior also occurs in the diode fault residual in Figure 17. To distinguish between the similar switching behavior of false alarms with real faults and to build confidence in the diagnostic algorithm, a fault will only be detected if the residual shows disagreement for at least 0.2 seconds. The belt fault will be detected at $t=38.4$ seconds. The diode fault will be detected at $t=10.7$ seconds. The controller fault will be detected at 10.2 seconds.

Isolation of a detected fault will be achieved by monitoring the switching behavior during a finite time window following detection. The belt fault appears in the residual when the load current increases or decreases. Due to the quick duration of load current change, the belt fault is also present for a short time in the residual lasting between two

to four seconds. The diode fault causes a large ripple in the alternator output current. This ripple causes frequent and rapid switching behavior from agreement to disagreement in the residual. The controller fault is the only fault case where there is residual disagreement for the entire duration of the fault. Therefore, the mean \bar{r} of the absolute value of the residuals during a finite time window can be used to isolate each fault as defined in Eq. (12). The time window is chosen based on data behavior. For the data in this paper, a six second window was used. Table 3 shows the mean value calculations for each fault using the six second window immediately after fault detection.

$$\bar{r} = \frac{\sum_{i=1}^n |r_i|}{n} \quad (12)$$

Table 3. Mean \bar{r} for six second window

Fault	Mean \bar{r}
Belt Slip	0.75
Open Diode	0.08
Voltage Controller	1

Appropriate constant thresholds for \bar{r} can isolate the fault. For this paper, if \bar{r} is between 0.5 and 1 the fault is due to belt slip. If \bar{r} is 1 the fault is due to the controller. Otherwise, the fault is due to an open diode.

Based on this approach, the belt fault will be isolated at $t=44.4$ seconds; the diode fault will be isolated at $t=16.7$ seconds; the controller fault will be isolated at time $t=16.3$ seconds.

Different fault magnitudes might require different isolation thresholds. This paper only considers three discrete fault modes.

7. CONCLUSION

This paper presents a novel method for calculating a time-varying probability transition matrix L for a quantized nonlinear system with the purpose of fault detection and isolation. Matrix L exploits the linear state space system that approximates the nonlinear system thereby reducing computational effort. Simple comparison of most probable state transitions from L and the quantized output states over time leads to fault detection and isolation. The merit of using matrix L for diagnostics is shown through the successful application of fault isolation in a 2D quantized alternator system.

ACKNOWLEDGEMENTS

Support for this research has been provided in part by the US Department of Energy GATE program and National Science Foundation under Grant No. 0825655.

Any opinions, findings, and conclusions or recommendations expressed in this material are those of the author(s) and do not necessarily reflect the views of the National Science Foundation.

NOMENCLATURE

ω_m	engine rotational speed
ω_e	alternator rotational speed
V_{dc}	battery DC voltage
V_f	field voltage
V_{ref}	voltage controller reference
I_{dc}	alternator output current
I_{load}	vehicle load current
I_B	battery charging current
z_1	first state space state
z_2	second state space state and output
u	state space input
$a(\omega_e)$	state space parameter dependent on alternator rotational speed
$b(\omega_e)$	state space parameter dependent on alternator rotational speed
z	current state
z'	possible future state
z_1^{\min}	minimum z_1 value
z_1^{\max}	maximum z_1 value
z^*	flow transition point on z_1 axis on side 1 of state z
z^{**}	flow transition point on z_1 axis on side 2 of state z
$z_2^{(1)}$	upper boundary of state z
$z_2^{(2)}$	lower boundary of state z
ϕ^+	flow up
ϕ^-	flow down
f	general function
\vec{F}	Field vector
\vec{n}	normal vector
C	general closed curve
A	area within curve C
r	line integral direction along curve C
ϕ_{in}	total flow into state z
ϕ_{out}	total flow out of state z
ϕ_{net}	net flow for given state z
z^+	state above state z
z^-	state below state z
L	time varying probability transition matrix
$[I_{dc}]$	quantized alternator output current
z_L	predicted future state using L
r	residual
\bar{r}	mean of absolute value of residual
n	number of data points

REFERENCES

Alam, M. & Lundstrom, M. (1995). Transition Matrix Approach for Monte Carlo Simulation of Coupled Electron/Phonon/Photon Dynamics, *Applied Physics Letters* (Vol 67. No. 4 pp. 512-514), July 24. doi: 10.1063/1.114553

Blanke, M., Kinnaert, M., Lunze, J., & Staroswiecki, M. (2006). *Diagnosis and Fault-Tolerant Control*. Germany: Springer.

Hashemi, A., & Pisu, P. (2011). Adaptive Threshold-based Fault Detection and Isolation for Automotive Electrical Systems (pp. 1013-1018), *World Congress on Intelligent Control and Automation*. June 21-25, Taipei, Taiwan. doi: 10.1109/WCICA.2011.5970668

Hashemi, A., & Pisu, P. (2011). Fault Diagnosis in Automotive Alternator System Utilizing Adaptive Threshold Method. *Annual Conference of Prognostics and Health Management Society*. September 25-29, Montreal, Canada.

Hashemi, A., (2011). *Model-Based System Fault Diagnosis Utilizing Adaptive Threshold with Application to Automotive Electrical Systems*. Masters dissertation. Clemson University, Clemson, South Carolina, USA. http://etd.lib.clemson.edu/documents/1314212419/Hashemi_clemson_0050M_11327.pdf

Scacchioli, A., Rizzoni, G., & Pisu, P., (2006). Model-Based Fault Detection and Isolation in Automotive Electrical Systems, *ASME International Mechanical Engineering Congress and Exposition* (pp. 315-324), November 5-10, Chicago, Illinois, USA. doi: 10.1115/IMECE2006-14504

Scacchioli, A., Li, W., Suozzo, C., Rizzoni, G., Pisu, P., Onori, S., Salman, M., Zhang, X., (2010). Experimental Implementation of a Model-Based Diagnosis for an electric Power Generation and Storage Automotive System, Submitted *ASME Tran. Dynamic Systems, Measurement, and Control*.

Scacchioli, A., Rizzoni, G., Salman, M., Onori, S., & Zhang, X. (2013). Model-based Diagnosis of an Automotive Electric Power Generation and Storage System. *IEEE Transaction on Human Machine Systems* (pp. 1-14), March 7. doi: 10.1109/TSMCC.2012.2235951

Zhang, X., Uliyar, H., Farfan-Ramos, L., Zhang, Y., & Salman, M. (2010). Fault Diagnosis of Automotive Electric Power Generation and Storage Systems, *IEEE International Conference on Control Applications* (pp. 719-724), September 8-10, Yokohama, Japan. doi: 10.1109/CCA.2010.5611179

Engineering from Clemson University (Clemson, SC, USA) in 2012. She is currently a Ph.D. student at Clemson University studying Automotive Engineering. She has completed summer internships at NASA Langley Research Center (Hampton, VA, USA) Thomas Jefferson National Accelerator Facility (Newport News, VA, USA), NOAA David Skaggs Research Center (Boulder, CO, USA), and Johns Hopkins University Applied Physics Laboratory (Laurel, MD, USA). She has completed a battery research project at BMW Manufacturing Company (Spartanburg, SC, USA) that resulted in filing a patent about methods to determine the condition of a battery. Her research interests are control, diagnostics, and prognostics for hybrid vehicles and electric vehicles. She is a member of ASME, SAE, SWE, and IEEE and received the national SEMA Top Student Award in 2012.



Pierluigi Pisu was born in Genoa, Italy in 1971. He received his Ph.D. in Electrical Engineering from Ohio State University (Columbus, Ohio, USA) in 2002. In 2004, he was granted two US patents in area of model-based fault detection and isolation. He is currently an Associate Professor in the Department of

Automotive Engineering at Clemson University and holds a joint appointment with the Department of Electrical and Computer Engineering at Clemson University. He is also a faculty member at the Clemson University International Center for Automotive Research. His research interests are in the area of fault diagnosis with application to vehicle systems, and energy management control of hybrid electric vehicles; he also worked in the area of sliding mode control and robust control. He is member of the ASME and SAE, and a recipient of the 2000 Outstanding Ph.D. Student Award by the Ohio State University Chapter of the Honor Society of Phi Kappa Phi.



Sara Mohon was born in Groton, Connecticut in 1987. She received her B.S. in Physics from the College of William and Mary (Williamsburg, VA, USA) in 2009 and M.S. in Automotive